Higher order multipolar polarizabilities of carbon tetrafluoride from isotropic and anisotropic light scattering experiments

3 AUTHORS:

M.S.A. El-Kader
Cairo University
45 PUBLICATIONS **111** CITATIONS

SEE PROFILE

Tadeusz Bancewicz
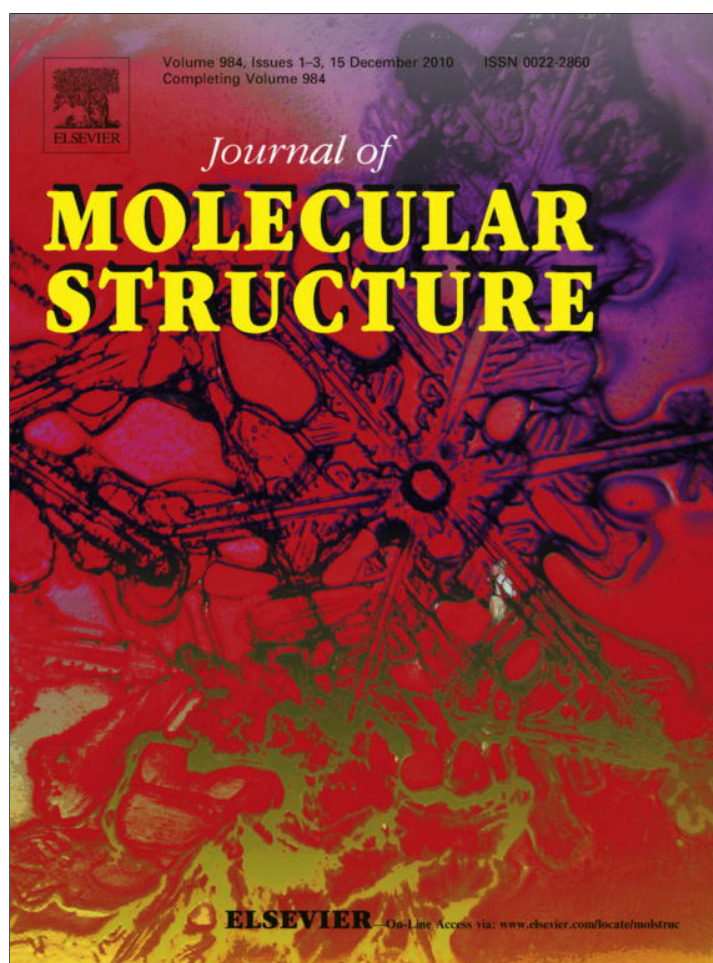Adam Mickiewicz University
58 PUBLICATIONS **590** CITATIONS

SEE PROFILE

George Maroulis
University of Patras
238 PUBLICATIONS **4,368** CITATIONS

SEE PROFILE

Higher order multipolar polarizabilities of carbon tetrafluoride from isotropic and anisotropic light scattering experiments

M.S.A. El-Kader [a,*], T. Bancewicz [b], G. Maroulis [c]

[a] Department of Engineering Mathematics and Physics, Faculty of Engineering, Giza 12211, Egypt
[b] Faculty of Physics, Department of Nonlinear Optics, Umultowska 85, 61-614 Poznan, Poland
[c] Department of Chemistry, University of Patras, Caratheodory St., GR-26500 Patras, Greece

ARTICLE INFO

ABSTRACT

The higher order dipole–quadrupole and dipole–octopole polarizabilities of carbon tetrafluoride has been determined from isotropic and anisotropic collision-induced light scattering (CILS) experiments of CF_4 and from anisotropic light scattering of its mixture with argon gas. The CILS spectra are analyzed by using the new updated and different intermolecular potentials. Our final estimates for these properties are $|\mathbf{A}| = (1.051 \pm 0.073)\ \text{Å}^4$ and $|\mathbf{E}| = (1.235 \pm 0.282)\ \text{Å}^5$ which are in excellent agreement with the *ab initio* theoretical values.

1. Introduction

Collision-induced light scattering (CILS) in fluids arises from polarizability variations caused by interactions between molecules [1]. For low-density fluids, interactions are binary and CILS comes from collisional polarizabilities of the molecular pairs. In the case of gases consisting of optically isotropic molecules, pure collision-induced anisotropic spectra are observed in the vicinity of the Rayleigh line where no monomolecular scattering is allowed [2,3]. Information on the molecular interactions may be obtained from these spectra. For the lower-frequency part of these collision-induced anisotropic spectra, the dipole-induced dipole (DID) interaction accounts for most of the observed scattering intensities, whereas, at high-frequency shifts, multipole polarizabilities have to be taken into account and play a leading role [3]. For isotropic molecules the excess polarizability induced by interactions in a pair is a tensor that has two invariants: its trace $\alpha(r)$ and its anisotropy $\beta(r)$ related to the translational isotropic and anisotropic CILS, respectively. For molecules it was proposed several years ago [3–5] that the dipole–quadrupole and dipole–octopole polarizabilities described by the tensors $\mathbf{A}$ and $\mathbf{E}$, respectively, contribute significantly to the high frequency scattering rotational spectrum.

In the case of carbon tetrafluoride (CF_4), the spectra consist essentially of an intense, pure translational component and a weaker induced rotational wing. Effects due to scattering by bound dimers [6–8] and to the quantum nature of the collision dynamics [9] are expected to become increasingly important to the translational component for this molecule. Induced rotational Raman scattering was first identified in the CF_4 spectrum [4]. It is a particularly propitious example in that the rotational wing clearly extends beyond the translational component over a broad frequency range, for this reason the two contributions may then be studied independently.

Different measurements of the isotropic and anisotropic light scattering intensities of this molecule from $2\ \text{cm}^{-1}$, up to $150\ \text{cm}^{-1}$ and anisotropic intensity of mixture of this molecule with argon atom from $4\ \text{cm}^{-1}$, up to $62\ \text{cm}^{-1}$ with a higher resolution, have been added for studying more closely the low-frequency part of the spectra (below $10\ \text{cm}^{-1}$, where discernible bound dimer features appear superimposed with the Raman transitions of the free pairs) [10–12]. Such a spectra, recorded at a temperature of 294.5 K will be analyzed here with the goal of developing refined models of the relevant interaction-induced properties, which permit an accurate reproduction of the observed spectra from lineshapes calculations. For all intensities and profiles calculations, the new updated and *ab initio* different intermolecular potentials [10,13–17] play an important role and the best available form must be chosen.

* Corresponding author.
  E-mail address: mohamedsay68@hotmail.com (M.S.A. El-Kader).

This paper assesses the validity of these models and the concomitant choice of parameter values in the description of the experimental spectra.

2. The intermolecular potential

In order to calculate the line profiles and their moments, the intermolecular potential is needed. Results with different potentials can be compared with experiment to assess the quality of the potential. The intermolecular potential we use is the HFD-B variety of Aziz and Chen [18].

The form of this potential is

$$V(r) = \varepsilon \left(A_0 \exp(-A_1(r/r_m) + A_2(r/r_m)^2) - F(r) \left(\sum_{i=0}^{2} \frac{C_{2i+6}}{(r/r_m)^{2i+6}} \right) \right) \tag{1}$$

with the damping function F given by

$$F(r) = \begin{cases} \exp(-(Dr/r_m - 1)^2) & r/r_m \leqslant D \\ 1 & \text{otherwise} \end{cases} \tag{2}$$

Even at the present HFD-B level, there are nine free parameters ε, A_0, A_1, A_2, r_m, D, C_6, C_8 and C_{10} which are far too many to determine from the present data. Accordingly we proceeded as follows: dispersion force constant C_6 is assumed known [19], C_8 and C_{10} are varied only from zero if the data cannot be fitted otherwise. Furthermore, in the initial fitting the parameters D, A_0, A_1 and A_2 were held fixed at some values while ε and r_m were chosen to minimize δ_B, δ_η, δ_λ, and $\delta_{D_{12}}$, the root mean square (rms) deviations calculated from the pressure second virial coefficient, viscosity, thermal conductivity and diffusion coefficient. This minimization is further supported by calculating δ_{M_0}, δ_{M_2} and δ_{M_4} the rms deviations calculated from the experimental zeroth, second and fourth moments of the anisotropic light scattering spectra.

This decision leads to potential 2 as shown in Table 1 with the parameters ε/k_B = 185.0 K, r_m = 5.05 Å and D = 1.645 for CF$_4$–CF$_4$ and ε/k_B = 163.5 K, r_m = 4.41 Å and D = 1.65 for CF$_4$–Ar interactions. They represent our best effort to determine the intermolecular potentials.

3. Calculations

In this section the calculations of the experimental quantities are described. The Monchick–Mason approximation [20] which neglects the effects of inelastic transitions on the relative kinetic energy is applied for check in the computation of the CILS profiles.

3.1. Analysis of pressure second virial coefficients

The pressure second virial coefficient B at temperature T was calculated classically from [21]

$$B(T) = 2\pi N_o \int_0^\infty [1 - \exp(-V(r)/k_B T)] r^2 \, dr \tag{3}$$

where N_o is the Avogadro number. The calculated $B(T)$ using the present HFD-B and other potentials were compared with the experimental results of Hurly [22] and Boushehri et al. [23] for CF$_4$–CF$_4$ and of Zarkova et al. [24] for CF$_4$–Ar which are seen in Figs. 1 and 2.

3.2. Analysis of traditional transport properties

The first check on the proposed potentials is to compare the transport properties i.e. viscosity (η), thermal conductivity (λ) and diffusion coefficient (D_{12}) at different temperatures of CF$_4$ and CF$_4$ with mixtures of Ar which are deduced using the formulas of Monchik et al. [20] and compared with the accurate experimental results of Boushehri et al. [23], Zarkova et al. [24], Hellemans [25], Uribe et al. [26], and Ketsin et al. [13].

3.3. The spectral lineshape and its moments

At moderate densities, the CILS spectra are determined by binary interactions. It consists of purely translational scattering which includes scattering due to free pairs and bound dimers, and the other is due to the induced rotational scattering. The pair polarizability trace and anisotropy giving rise to the translational scattering of the isotropic and anisotropic light spectra in the case of inert gases and spherical top molecules are given by the following formula [27]:

Table 1
Parameters of the trial HFD-B potentials and the associated values of δ^a. The number in parenthesis is the power of 10.

Potential parameters	CF$_4$–CF$_4$			CF$_4$–Ar		
	1	2	3	1	2	3
ε/k_B (K)	183.5	185.0	186.8	161.0	163.5	165.0
σ (Å)	4.535	4.528	4.520	4.0225	3.9915	3.9755
r_m (Å)	5.0611	5.050	5.0440	4.450	4.410	4.390
A_0	3.30741(6)	3.24924(6)	3.65739(6)	9.29844(6)	1.0791(7)	1.1323(7)
A_1	15.9	15.82	15.7	15.64	15.60	15.58
A_2	0.295614	0.241124	−0.040724	−1.28986	−1.50411	−1.5765
δ_B	0.75	0.67	0.73	0.25	0.20	0.40
δ_η	0.82	0.73	0.71	0.90	0.71	0.62
δ_λ	0.86	0.76	0.75	–	–	–
$\delta_{D_{12}}$	0.93	0.84	0.84	0.68	0.56	0.50
δ_{M_0}	0.97	0.94	0.95	1.35	1.42	1.53
δ_{M_2}	0.62	0.60	0.76	0.55	0.57	0.83
δ_{M_4}	0.58	0.47	0.78	0.75	0.074	0.44
δ_t	0.81	0.73	0.8	0.82	0.73	0.82

δ^a is defined by $\delta^a = \sqrt{(1/N)\left(\sum_{j=1}^{N}\left(1/n_j \sum_{j=1}^{n_j} \Delta_{ji}^{-2}(P_{ji} - p_{ji})^2\right)\right)}$, where P_{ji} and p_{ji} are, respectively, the calculated and experimental values of property j at point i and Δ_{ji} is the experimental uncertainty of property j at point i. The subscripts B, η, λ, D_{12}, M_0, M_2, M_4 and t refer, respectively, to the pressure second virial coefficient, the viscosity, the thermal conductivity, the mixtures diffusion coefficient, the zeroth, second and fourth spectral moments and total.
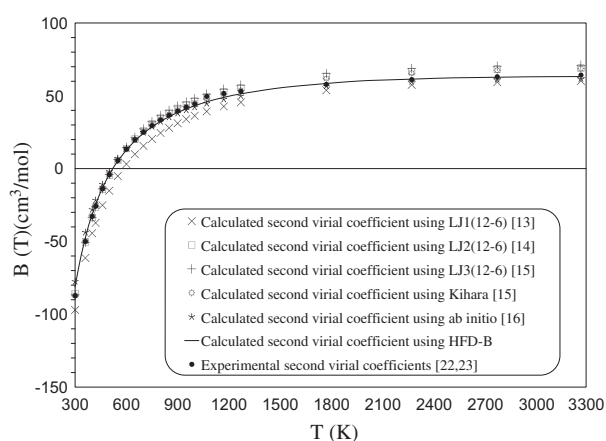
Fig. 1. CF$_4$–CF$_4$ pressure second virial coefficients in cm^3 mol^{-1} versus temperature in K. Points refer to the experiments [22,23]. The calculations were performed using LJ1(12-6), LJ2(12-6), LJ3(12-6) potentials [13–15], Kihara potential [15], *ab initio* potential [16] and our new HFD-B one given in Table 1 and labeled 3.
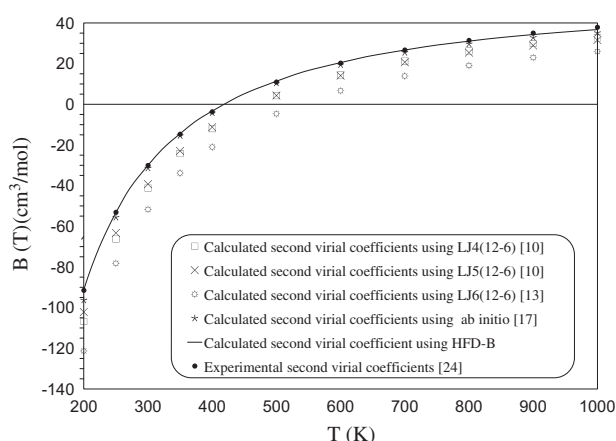

Fig. 2. CF$_4$–Ar pressure second virial coefficients in cm^3 mol^{-1} versus temperature in K. Points refer to the experiments [24]. The calculations were performed using LJ4(12-6), LJ5(12-6), LJ6(12-6) potentials [10,13], *ab initio* potential [17] and our new HFD-B one given in Table 1 and labeled 3.

$$\alpha(r) = \frac{\left(2\alpha_1\alpha_2^2 + 2\alpha_1^2\alpha_2 + 5C_6\left(\frac{\gamma_1}{18\alpha_1} + \frac{\gamma_2}{18\alpha_2}\right)\right)}{r^6} + \frac{20\alpha_1\alpha_2\sqrt{C_1C_2}}{r^8}$$
$$- t_o \exp\left(-\frac{r-\sigma}{r_t}\right) \tag{4}$$

$$\beta(r) = \frac{6\alpha_1\alpha_2}{r^3} + \frac{\left(3\alpha_1\alpha_2^2 + 3\alpha_1^2\alpha_2 + C_6\left(\frac{\gamma_1}{6\alpha_1} + \frac{\gamma_2}{6\alpha_2}\right)\right)}{r^6}$$
$$+ \frac{24\alpha_1\alpha_2\sqrt{C_1C_2}}{r^8} - g_o \exp\left(-\frac{r-\sigma}{r_o}\right) \tag{5}$$

α_1 and α_2 are the polarizabilities, γ_1 and γ_2 are the second hyperpolarizabilities, C_1 and C_2 are the quadrupole polarizabilities of CF$_4$ and Ar. Values of the polarizabilities used in Eqs. (4) and (5) are given in Table 2. The coefficients C_6 and σ were determined from the expression for the potentials.

A purely long-range interaction mechanism, involving the participation of high order polarizabilities, has been invoked to account for induced rotational scattering [4]. Contributions from the dipole–quadrupole (**A**) and dipole–octopole (**E**) polarizabilities for CF$_4$ symmetry give the intensity of the observed rotational

Table 2
Polarizabilities and different parameters used in calculations.

	CF$_4$	Ar	CF$_4$–CF$_4$	CF$_4$–Ar
α (a.u.)	19.51 [28,29]	10.66 [30]	–	–
γ (a.u.)	978 [28,29]	942 [31]	–	–
C (a.u.)	126.49 [28,29]	49.70 [32]	–	–
g_o (a.u.)	–	–	0.70858	0.5911546
r_o (a.u.)	–	–	0.801244105	0.595264
t_o (a.u.)	–	–	0.320546	–
r_t (a.u.)	–	–	0.755891	–

spectra with the predictions of the mean square polarizability models in the case of the isotropic and anisotropic spectra as

$$\langle \alpha_{zz}^2 \rangle = (\alpha_1 + \alpha_2)^2 + \frac{16}{5}(\alpha_1\alpha_2)^2 r^{-6} + \frac{592}{105}((\alpha_1\mathbf{A}_2)^2$$
$$+ (\alpha_2\mathbf{A}_1)^2)r^{-8} + \frac{52}{9}((\alpha_1\mathbf{E}_2)^2 + (\alpha_2\mathbf{E}_1)^2)r^{-10} + \frac{95616}{4725}$$
$$\times (\mathbf{A}_1\mathbf{A}_2)^2 r^{-10} + \frac{344}{21}((\mathbf{A}_1\mathbf{E}_2)^2 + (\mathbf{A}_2\mathbf{E}_1)^2)r^{-12} + \frac{8591}{105}$$
$$\times ((\mathbf{E}_1\mathbf{E}_2)^2)r^{-14} + \cdots, \tag{6}$$

$$\langle \alpha_{xz}^2 \rangle = \frac{12}{5}\alpha_1^4 r^{-6} + \frac{96}{35}((\alpha_1\mathbf{A}_1)^2)r^{-8} + \frac{22}{9}((\alpha_1\mathbf{E}_1)^2)r^{-10}$$
$$+ \frac{62912}{4725}((\mathbf{A}_1^4)r^{-10} + \frac{464}{21}((\mathbf{A}_1\mathbf{E}_1)^2)r^{-12}$$
$$+ \frac{5863}{105}(\mathbf{E}_1^4)r^{-14} + \cdots \tag{7}$$

for CF$_4$–CF$_4$ interactions

$$\langle \alpha_{zz}^2 \rangle = (\alpha_1 + \alpha_2)^2 + \frac{16}{5}(\alpha_1\alpha_2)^2 r^{-6} + \frac{592}{105}((\alpha_2\mathbf{A}_1)^2)r^{-8} + \frac{52}{9}$$
$$\times ((\alpha_2\mathbf{E}_1)^2)r^{-10} + \cdots, \tag{8}$$

$$\langle \alpha_{xz}^2 \rangle = \frac{12}{5}(\alpha_1\alpha_2)^2 r^{-6} + \frac{48}{35}((\alpha_2\mathbf{A}_1)^2)r^{-8} + \frac{11}{9}((\alpha_2\mathbf{E}_1)^2)r^{-10} + \cdots \tag{9}$$

for CF$_4$–Ar interactions

The angular brackets $\langle \cdots \rangle$ denote an average over all orientations of the intermolecular and molecular axes.

The various terms in Eqs. (6)–(9) give rise to the following selection rules on J the total angular momentum quantum number:

$\alpha_i\mathbf{A}_j$,	$\Delta J_i = 0$,	$\Delta J_j = 0, \pm 1, \pm 2, \pm 3$,	$J_j + J_j' \geqslant 3$
$\alpha_i\mathbf{E}_j$,	$\Delta J_i = 0$,	$\Delta J_j = 0, \pm 1, \pm 2, \pm 3, \pm 4$	$J_j + J_j' \geqslant 4$
$\mathbf{A}_i\mathbf{A}_j$,	$\Delta J_i = 0, \pm 1, \pm 2, \pm 3$,	$\Delta J_j = 0, \pm 1, \pm 2, \pm 3$,	$J_i + J_i' \geqslant 3$
			$J_j + J_j' \geqslant 3$
$\mathbf{A}_i\mathbf{E}_j$,	$\Delta J_i = 0, \pm 1, \pm 2, \pm 3$,	$\Delta J_j = 0, \pm 1, \pm 2, \pm 3, \pm 4$	$J_i + J_i' \geqslant 3$
			$J_j + J_j' \geqslant 4$
$\mathbf{E}_i\mathbf{E}_j$,	$\Delta J_i = 0, \pm 1, \pm 2, \pm 3, \pm 4$	$\Delta J_j = 0, \pm 1, \pm 2, \pm 3, \pm 4$	$J_i + J_i' \geqslant 4$
			$J_j + J_j' \geqslant 4$

The quantum theory is applied for the accurate computation of the CILS absolute translational intensities of the tetrafluoromethane pairs and of the tetrafluoromethane with argon. Numerically, this is done by means of the propagative two-point Fox–Goodwin integrator [33,34], where the ratio of the wavefunction, defined at adjacent points on a spatial grid, is built step-by-step.

As regards our problem, binary isotropic and anisotropic light scattering spectra are computed quantum-mechanically, as a function of frequency shifts v, at temperature T by using the expressions [35–38]:

$$I_{iso}(v) = hc\lambda^3 k_s^4 \sum_{J=0,J\,even}^{J_{max}} (2J+1) \int_0^{E_{max}} |\langle \psi_{E'J'}|\alpha|\psi_{EJ}\rangle|^2 \exp\left(-\frac{E}{k_BT}\right) dE \tag{10}$$

$$I_{aniso}(v) = \frac{2}{15} hc\lambda^3 k_s^4 \sum_{J=0,J\,even}^{J_{max}} g_J b_J^{J'} (2J+1) \int_0^{E_{max}} |\langle \psi_{E'J'}|\beta|\psi_{EJ}\rangle|^2 \exp\left(\frac{-E}{k_BT}\right) dE \tag{11}$$

The symbol k_s stands for the Stokes wave number of the scattered light, h is Planck's constant and c is the speed of the light. Constant λ account for the thermal de Broglie wavelength, $\lambda = h/\sqrt{2\pi\mu k_BT}$, with μ the reduced mass of (CF_4 and CF_4) in case of pure gases, (CF_4 and Ar) in case of mixture and k_B Boltzmann's constant. Symbol ψ_{EJ} designates the scattering wave function and E_{max} the maximum value of the energy that is required to obtain convergence of the integrals.

In these expressions, $\alpha = \alpha(r)$ and $\beta = \beta(r)$ denote the trace and anisotropy of the quasimolecule, g_J the nuclear statistical weight and $b_J^{J'}$ are intensity factors involving the rotational quantum numbers J and J' of the initial and final states, respectively.

With the spectral intensities $I_{iso}(v)$ and $I_{aniso}(v)$ in cm^6 as input and through the following analytical expressions we are able to deduce the isotropic and anisotropic moments [39–41]

$$M_0^{iso} = 4\pi \int_0^\infty \alpha^2(r) \exp(-V(r)/k_BT) r^2\, dr \tag{12}$$

$$M_2^{iso} = \frac{4\pi k_BT}{\mu} \int_0^\infty \left(\frac{d\alpha(r)}{dr}\right)^2 \exp(-V(r)/k_BT) r^2\, dr \tag{13}$$

$$
\begin{aligned}
M_4^{iso} = 4\pi\left(\frac{k_BT}{\mu}\right)^2 \int_0^\infty & \exp(-V(r)/k_BT)\left(3\left(\frac{d^2\alpha(r)}{dr^2}\right)^2\right. \\
& + \frac{4}{r}\left(\frac{d^2\alpha(r)}{dr^2}\right)\left(\frac{d\alpha(r)}{dr}\right) + \frac{8}{r^2}\left(\frac{d\alpha(r)}{dr}\right)^2 \\
& - 2\left(\frac{d\alpha(r)}{dr}\right)\left(\frac{dV(r)/dr}{k_BT}\right)\left(\left(\frac{d^2\alpha(r)}{dr^2}\right)\right) \\
& \left. + \frac{2}{r}\left(\frac{d\alpha(r)}{dr}\right)\right) + \left(\left(\frac{d\alpha(r)}{dr}\right)^2\right)\left(\frac{dV(r)/dr}{k_BT}\right)^2\right) r^2\, dr
\end{aligned}
\tag{14}
$$

$$M_0^{aniso} = 4\pi \int_0^\infty \beta^2(r) \exp(-V(r)/k_BT) r^2\, dr \tag{15}$$

$$M_2^{aniso} = \frac{4\pi k_BT}{\mu} \int_0^\infty \left(\left(\frac{d\beta}{dr}\right)^2 + 6\left(\frac{\beta}{r}\right)^2\right) \exp(-V(r)/k_BT) r^2\, dr \tag{16}$$

$$
\begin{aligned}
M_4^{aniso} = \int_0^\infty & \left(4\pi\left(\frac{k_BT}{\mu}\right)^2\left(3\left(\frac{d^2\beta}{dr^2}\right)^2 + \frac{4}{r}\left(\frac{d\beta}{dr}\right)\left(\frac{d^2\beta}{dr^2}\right)\right.\right. \\
& - 12\frac{\beta}{r^2}\left(\frac{d^2\beta}{dr^2}\right) + \frac{32}{r^2}\left(\frac{d\beta}{dr}\right)^2 - 96\frac{\beta}{r^3}\left(\frac{d\beta}{dr}\right) + 120\frac{\beta^2}{r^4}\right) \\
& - 4\pi\frac{2k_BT}{\mu}\left(\frac{1}{\mu}\left(\frac{dV}{dr}\right)\left(\frac{d\beta}{dr}\right)\left(\left(\frac{d^2\beta}{dr^2}\right) + \left(\frac{2}{r}\right)\left(\frac{d\beta}{dr}\right)\right.\right. \\
& \left.\left.\left. - 6\left(\frac{\beta}{r^2}\right)\right)\right) + 4\pi\left(\frac{1}{\mu}\right)^2 + \left(\frac{dV}{dr}\right)^2\left(\frac{d\beta}{dr}\right)^2\right) \exp(-V(r)/k_BT) r^2\, dr
\end{aligned}
\tag{17}
$$

where λ denotes the laser wavelength and $V(r)$ is the interatomic potential.

Throughout this paper the calculated values of the spectral moments reported are obtained numerically from quantum expressions (correct to order $\hbar^2$) that involve the equilibrium pair correlation function, the potential and the collision-induced trace and anisotropy pair polarizability.

These results were compared with the experimental moments obtained from the isotropic and anisotropic intensities of the light scattering spectra,

$$M_{2n}^{iso} = \left(\frac{\lambda_o}{2\pi}\right)^4 \int_{-\infty}^\infty (2\pi cv)^{2n} I_{iso}(v)\, dv \tag{18}$$

$$M_{2n}^{aniso} = \frac{15}{2}\left(\frac{\lambda_o}{2\pi}\right)^4 \int_{-\infty}^\infty (2\pi cv)^{2n} I_{aniso}(v)\, dv \tag{19}$$

The total theoretical intensities of the isotropic and anisotropic light scattering spectra are the sum of the translational spectra due to the transitions of bound–bound, bound–free and free–free states and rotational spectra.
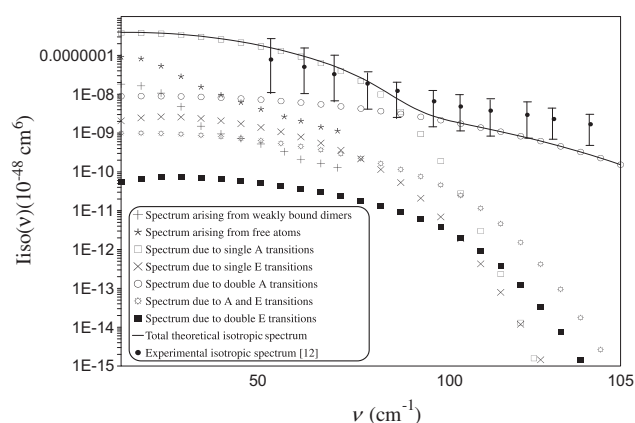

Fig. 3. Intensity of the two-body isotropic light scattering spectrum of CF_4-CF_4 at $T = 294.5$ K plotted as a function of frequency shifts. Calculations were performed with our empirical HFD-B intermolecular potential given in Table 1 and labeled 2. Theoretical curves are provided for several contributions using $\alpha_1 = 2.937$ Å^3, **A** = 0.92 Å^4 and **E** = 1.103 Å^5.

Fig. 4. Intensity of the two-body anisotropic light scattering spectrum of CF_4–CF_4 at $T = 294.5$ K plotted as a function of frequency shifts. Calculations were performed with our empirical HFD-B intermolecular potential given in Table 1 and labeled 2. Theoretical curves are provided for several contributions using $\alpha_1 = 2.937$ Å^3, **A** = 1.051 Å^4 and **E** = 1.235 Å^5.
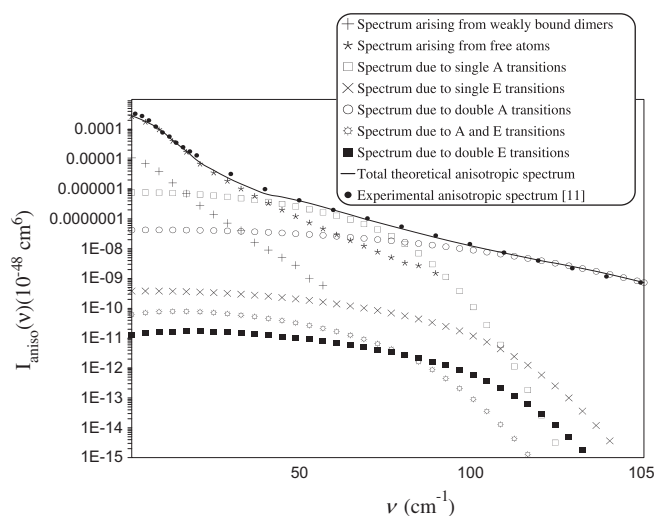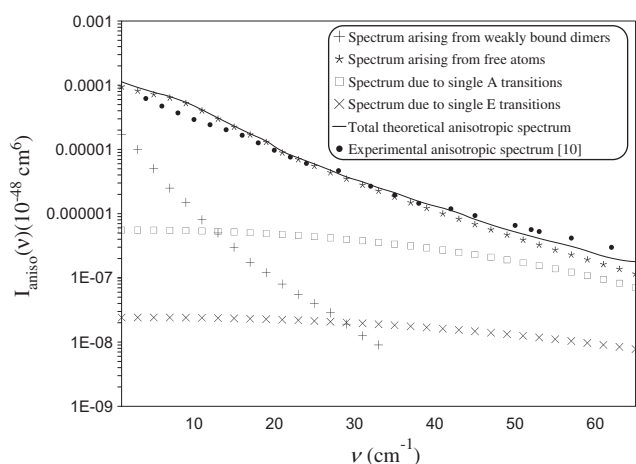
Fig. 5. Intensity of the two-body anisotropic light scattering spectrum of CF_4–Ar at $T = 294.5$ K plotted as a function of frequency shifts. Calculations were performed with our empirical HFD-B intermolecular potential given in Table 1 and labeled 2. Theoretical curves are provided for several contributions using $\alpha_1 = 2.937$ Å^3, $\alpha_2 = 1.679$ Å^3, **A** = 1.34 Å^4 and **E** = 1.88 Å^5.

In order to calculate the line profiles and the associated moments, the intermolecular potential is needed. Results with different potentials can be compared with experiment to asses the quality of the potential. In this paper we consider the different empirical and recent *ab initio* potentials [10,13–17].

Comparisons between the calculations and experiments are shown in Figs. 3–5 for the intensities of the isotropic and anisotropic light scattering spectra, and Table 3 for the first few even moments of the anisotropic profiles.

Concerning the multipolar contributions of single **A**, double **A**, single **E**, **A** and **E** and double **E** transitions, different values of the dynamic independent tensor components **A** and **E** may be used to fit the experimental isotropic and anisotropic intensities in the frequency ranges 50–180 cm^{-1} and 30–62 cm^{-1} for CF_4 and CF_4 with Ar respectively. Figs. 3–5 suggest that there are a choices of **A** and **E** for which the theoretical and experimental isotropic and anisotropic spectra fit the best $|\mathbf{A}| = 0.92$ Å^4, 1.051 Å^4 and $|\mathbf{E}| = 1.103$, 1.235 Å^5 for CF_4–CF_4 and $|\mathbf{A}| = 1.34$ Å^4, $|\mathbf{E}| = 1.88$ Å^5 for CF_4–Ar using the our empirical HFD-B interatomic potentials. Also in Table 4 we have reported the theoretical and experimental values of these coefficients from the bond polarizability model and molecular beam scattering [3,41] and those calculated *ab initio* by Maroulis (i.e., his "best or recommended" SCF and MP_4 values taking into account electron correlation corrections) [28,29].

In Table 2 our models of the interatomic potentials are compared with the recent *ab initio* potentials [16,17]. Good agreement between these models and the *ab initio* ones is generally observed and the calculated profiles agree with the measurements at $T = 294.5$ K as shown in Figs. 3–5.

It is immediately apparent from the comparison in Tables 3 and 4 that our HFD-B potentials are better than LJ2-5 [10,13,14,17] potentials. Also, it is better than that previously available, where the spectral profiles calculated with Kihara model [15].

Table 3
Different contributions from bound (*B*), free (*F*), rotational (*R*) and total (*T*) anisotropic zeroth-order M_0, second-order M_2 and fourth-order M_4 moments at $T = 294.5$ K deduced from experiment and theory using different intermolecular potential models.

Moments potential	M_0 (Å^9) Experimental				M_2 (Å^9/S^2) Experimental				M_4(Å^9/S^4) Experimental			
	CF$_4$–CF$_4$ 148.36 ± 25 [10] 182 ± 24 [11] CF$_4$–Ar 57.58 ± 7.5 [10] Calculated				CF$_4$–CF$_4$ 407.1 ± 23 [10] CF$_4$–Ar 368.74 ± 26 [10] Calculated				CF$_4$–CF$_4$ 13804.42 ± 2512 [10] CF$_4$–Ar 19965.35 ± 6000 [10] Calculated			
	B	*F*	*R*	*T*	*B*	*F*	*R*	*T*	*B*	*F*	*R*	*T*
CF$_4$–CF$_4$ LJ2 [14]	19.2	126.54	3.4	149.12	7.14	284.8	104.7	396.7	39.7	5079.1	8877.4	13996.0
Kihara [15]	43.4	123.1	2.24	168.75	33.85	277.4	80.14	391.4	32.97	4741.0	9506.1	14576.8
Abinitio [16]	40.62	128.0	2.17	170.77	30.4	291.7	77.98	400.1	44.7	4462.8	9319.8	13827.3
HFD-B	28.52	131.58	2.17	162.27	22.9	308.4	77.98	409.28	236.6	5233.6	8369.6	13839.8
CF$_4$–Ar LJ4 [10]	5.81	45.17	9.13	60.11	3.12	169.94	290.3	463.36	39.83	4986.8	24831.	29857.0
LJ5 [10]	8.96	69.86	3.81	82.63	7.57	368.53	122.0	498.1	418.9	16807.	10542.	27768.0
Abinitio [17]	12.4	66.1	1.53	80.1	12.3	363.4	49.0	424.7	231.2	15808.	4261.4	20069.4
HFD-B	10.3	66.7	1.5	78.5	10.3	319.5	47.0	376.8	393.6	15342.8	4261.4	19997.8

Table 4
Values of the independent components **A** and **E** of the dipole–quadrupole and dipole–octopole polarizability tensors, respectively, for the CF_4 molecule.

Method	Potential	$|\mathbf{A}|$ (Å^4)	$|\mathbf{E}|$ (Å^5)	Reference
Theory				
Ab initio (SCF)		0.97	1.15	[28,29]
Bond polarizability model		2.2	3.5	[3]
Molecular beam scattering		⩽2.2	⩽10	[41]
Anisotropic light scattering of CF$_4$–CF$_4$	LJ2(12-6) [14]	2.2	2.2	[10]
Anisotropic light scattering of CF$_4$–Ar	LJ4(12-6) [10]	6.0	6.0	[10]
Anisotropic light scattering of CF$_4$–Ar	LJ5(12-6) [10]	2.8	2.8	[10]
Anisotropic light scattering of CF$_4$–CF$_4$	LJ2(12-6) [14]	0.5–1.7	2.5–4.3	[11]
Anisotropic light scattering of CF$_4$–CF$_4$	Kihara [15]	0.4–1.4	1.4–3.3	[12]
Isotropic light spectrum of CF$_4$–CF$_4$	LJ3(12-6) [15]	0.5–1.2	1.0–3.5	[12]
Isotropic spectrum of CF$_4$–CF$_4$	HFD-B	0.92 ± 0.064	1.103 ± 0.252	This work
Anisotropic spectrum of CF$_4$–CF$_4$	HFD-B	1.051 ± 0.073	1.235 ± .0282	This work
Anisotropic spectrum of CF$_4$–Ar	HFD-B	1.327 ± 0.0376	1.51 ± 0.287	This work

4. Conclusion

The present study further demonstrates that the empirical HFD-B potential models are a very good representation of the intermolecular potential of gaseous CF_4 and of CF_4 with Ar. The profiles of the two-body anisotropic collision-induced light scattering spectra at $T = 294.5$ K can be accounted for by a calculation employing a classical trajectory to simulate the collision. The significant contributions to the spectra by bound dimers are found to be essentially the same as that arrived at by a full quantum mechanical calculations. At high frequencies we show that most of the intensities may be attributed to multipolar contributions involving the dipole–quadrupole **A** and dipole–octopole **E** polarizability tensors. Moreover, the very broad frequency range probed by Bancewicz et al. provides enough information to deduce values for the independent components of **A** and **E**, this is confirmed by the good agreement between our fitted values from spectra and the one computed *ab initio* by Maroulis [28,29]. In conclusion, this work shows that when high frequency intensities are observed CILS is a suitable technique for studying multipolar contributions in a tetrahedral molecule.

References

[1] G.C. Tabisz, M.N. Neuman (Eds.), Collision- and Interaction-Induced Spectroscopy, NATO Advanced Study Institute, Series C: Mathematical and Physical Science, vol. 452, Kluwer, Dordrecht, 1995.
[2] A.T. Prengel, W.S. Gormall, Phys. Rev. A13 (1976) 253.
[3] A.D. Buckingham, G.C. Tabisz, Mol. Phys. 36 (1978) 583.
[4] A.D. Buckingham, G.C. Tabisz, Opt. Lett. 1 (1977) 220.
[5] H.A. Posch, Mol. Phys. 46 (1982) 1213.
[6] N. Meinander, G.C. Tabisz, M. Zoppi, J. Chem. Phys. 84 (1986) 3005.
[7] D.H. Godfried, I.F. Silvera, Phys. Rev. Lett. 48 (1982) 1337. Phys. Rev. A 27 (1982) 3008.
[8] Y. Le Duff, R. Ouillon, V. Chandrasekharan, B. Silvi, Mol. Phys. 62 (1987) 1065.
[9] F. Barocchi, M. Moraldi, M. Zoppi, J.D. Poll, Mol. Phys. 43 (1981) 1193.
[10] S.M. El-Sheikh, G.C. Tabisz, Mol. Phys. 68 (1989) 1225.
[11] A. Elliasmine, J.-L. Godet, Y. Le Duff, T. Bancewicz, Mol. Phys. 90 (1997) 147.
[12] A. Elliasmine, J.-L. Godet, Y. Le Duff, T. Bancewicz, Phys. Rev. A55 (1997) 4230.
[13] J. Kestin, H.E. Khalifa, S.T. Ro, W.A. Wakeham, Physica A88 (1977) 242.
[14] K.E. MacCormack, W.G. Schneider, J. Chem. Phys. 19 (1951) 849.
[15] A.E. Sherwood, J.M. Prausnitz, J. Chem. Phys. 41 (1964) 429.
[16] R. Mahlanen, J.-P. Jalkanen, T.A. Pakkanen, Chem. Phys. 313 (2005) 271.
[17] G. Vayner, Y. Alexeev, J. Wang, T.L. Windus, W.L. Hase, J. Phys. Chem. A 110 (2006) 3174.
[18] R.A. Aziz, H.H. Chen, J. Chem. Phys. 67 (1977) 5719.
[19] R.T. Pack, J.J. Valentini, C.H. Becker, R.J. Buss, Y.T. Lee, J. Chem. Phys. 77 (1982) 5475.
[20] L. Monchick, K.S. Yun, E.A. Mason, J. Chem. Phys. 39 (1963) 654.
[21] J.H. Dymond, E.B. Smith, The Virial Coefficients of Pure Gases and Mixtures, Oxford University, Oxford, 1980.
[22] J.J. Hurly, Int. J. Thermophys. 20 (1999) 455.
[23] A. Boushehri, J. Bzowski, J. Kestin, E.A. Mason, J. Phys. Chem. Ref. Data 16 (3) (1987) 445.
[24] L. Zarkova, U. Hohm, M. Damyanova, J. Phys. Chem. Ref. Data 32 (4) (2003) 1639.
[25] J.M. Hellemans, Physica 65 (1973) 376.
[26] F.J. Uribe, E.A. Mason, E.A. Kestin, J. Phys. Chem. Ref. Data 19 (1990) 1123.
[27] S.M. El-Sheikh, G.C. Tabisz, A.D. Buckingham, Chem. Phys. 247 (1999) 407.
[28] G. Maroulis, Chem. Phys. Lett. 259 (1996) 654.
[29] G. Maroulis, J. Chem. Phys. 105 (1996) 8467.
[30] A. Dalgrano, A.E. Kingston, Proc. Roy. Soc. A 259 (1960) 424.
[31] A.D. Buckingham, D.A. Dunmur, Trans. Faraday Soc. 64 (1968) 1776.
[32] G. Maroulis, J. Phys. Chem. A 104 (2000) 4772.
[33] D.W. Norcross, M.J. Seaton, J. Phys. B6 (1973) 614.
[34] M. Chrysos, R. Lefebvre, J. Phys. B 26 (1993) 2627.
[35] N. Meinander, in: L. Frommhold, J.W. Keto (Eds.), Spectral Line Shapes, vol. 6, AIP, New York, 1990, p. 515.
[36] O. Gaye, M. Chrysos, V. Teboul, Y. Le Duff, Phys. Rev. A55 (1997) 3484.
[37] M. Chrysos, O. Gaye, Y. Le Duff, J. Phys. B 29 (1996) 583.
[38] M. Chrysos, O. Gaye, Y. Le Duff, J. Chem. Phys. 105 (1996) 1.
[39] H.B. Levine, G. Birnbaum, J. Chem. Phys. 55 (1971) 2914.
[40] C.G. Joslin, J.D. Goddard, S. Goldman, Mol. Phys. 89 (3) (1996) 791.
[41] U. Bafile, R. Magli, F. Barocchi, M. Zoppi, L. Frommhold, Mol. Phys. 49 (1983) 1149.